J Mater Sci (2009) 44:385–391
DOI 10.1007/s10853-008-3149-1

Crystallization kinetic studies of $CaBi_2B_2O_7$ glasses by non-isothermal methods

Koushik Majhi · K. B. R. Varma

Received: 25 July 2008 / Accepted: 1 December 2008 / Published online: 16 December 2008

Abstract Transparent glasses of $CaBi_2B_2O_7$ (CBBO) were fabricated via the conventional melt-quenching technique. The amorphous and the glassy nature of the as-quenched samples were, respectively, confirmed by X-ray powder diffraction (XRD) and differential scanning calorimetry (DSC). The glass transition (T_g) and the crystallization parameters (crystallization activation energy (E_{cr}) and Avrami exponent (n)) were evaluated under non-isothermal conditions using DSC. The heating rate dependent glass transition and the crystallization temperatures were rationalized by Lasocka equation for the as-quenched CBBO glasses. There was a close agreement between the activation energies for the crystallization process determined by Augis and Bennet and Kissinger methods. The variation of local activation energy ($E_c(x)$) that was determined by Ozawa method increased with the fraction of crystallization (x). The Avrami exponent ($n(x)$) decreased with the increase in fraction of crystallization (x), suggesting that there was a changeover in the crystallization process from the bulk to the surface.

Introduction

Glasses comprising non-linear optical crystals have been of increasing interest for a variety of applications. For instance, transparent crystallized glasses of $LaBGeO_5$, $SrBi_2Ta_2O_9$, $SrBi_2Nb_2O_9$, which are important from their multifunctionalities viewpoint, have been fabricated and characterized [1–3]. Recently, $CaBi_2B_2O_7$ (CBBO) was reported to be belonging to orthorhombic crystal system associated with $Pna2_1$ polar space group [4]. Since it is polar, we thought it is worth fabricating transparent glasses of CBBO embedded with nano/microcrystallites of the same composition and examine their physical properties as these composites have great potential for device applications. To begin with, we aimed at understanding the crystallization kinetics as these provide a priori knowledge about optimization of certain parameters that are important in the fabrication of optical glass nano/microcrystal composites.

Differential thermal analysis (DTA) and differential scanning calorimetry (DSC) could frequently be used to study the crystallization kinetics of the glassy materials [5–9]. For determining the kinetic parameters such as the activation energy of crystallization (E_{cr}) and Avrami exponent (n) in Johnson–Mehl–Avrami (JMA) equation [10–12], for the present CBBO glasses, non-isothermal methods are employed. The activation energy associated with the glass transition is determined using Kissinger [13] and Moynihan [14] methods. Heating rate dependent glass transition and crystallization temperatures are rationalized using Lascoka equation [15]. Also, the variations of activation energy and Avrami exponent with the fraction of crystallization are examined. The details of which are reported in this article.

Experimental

CBBO glasses were fabricated via the conventional melt-quenching technique. For this, the reagent grade $CaCO_3$ (99.95%, Aldrich), Bi_2O_3 (99.9%, Merck), and B_2O_3 (99.9%, Aldrich) in molar ratio (to yield $CaBi_2B_2O_7$ phase)

K. Majhi · K. B. R. Varma (✉)
Materials Research Centre, Indian Institute of Science, Bangalore 560 012, India
e-mail: kbrvarma@mrc.iisc.ernet.in

were mixed and melted in a platinum crucible at 1373 K for 1 h. Melts were quenched by pouring on a steel plate and pressed with another plate to obtain 1–1.5 mm thick glass plates. X-ray powder diffraction (XRD) studies were performed using Philips PW1050/37 diffractometer (Cu-K_α radiation) to confirm the amorphous and crystalline nature of the as-quenched and heat-treated glasses, respectively. The DSC (Model: Diamond DSC, Perkin-Elmer) runs were carried out in the 550–900 K temperature range. For glass transition analysis, the sample was heated and cooled from 655 to 770 K at different heating rates (10, 15, 20, and 25 K/min). For non-isothermal experiments, the glass samples were heated from 800 to 900 K at the rate of 10, 15, 20, and 25 K/min. All the experiments were conducted in dry nitrogen ambience. The as-quenched glass plates weighing 15 mg were used for all the experiments.

Results and discussion

The XRD patterns obtained for the as-quenched and heat-treated CBBO glass plates are shown in Fig. 1a and b. The as-quenched samples were confirmed to be amorphous (Fig. 1a). Figure 2 shows the typical DSC trace recorded for the as-quenched CBBO glass plate at a heating rate of 10 K/min. An endotherm around 686 K followed by an exotherm at 825 K associated with the glass transition (T_g), and the onset of the crystallization temperature (T_{cr}), respectively, for the as-quenched sample are observed. The peak glass transition temperature (T_{gp}) is the temperature at which it attains a maximum in the DSC curves. There is an upward shift in the T_{gp} with an increasing heating rate (α). The heat-treated (875 K/12 h > T_{cr} in DSC studies) sample reveals its crystalline nature (Fig. 1b). All the Bragg peaks in this pattern could be indexed to an orthorhombic phase of $CaBi_2B_2O_7$, suggesting that these glasses undergo bulk crystallization process. No impurity or secondary phases are detectable.

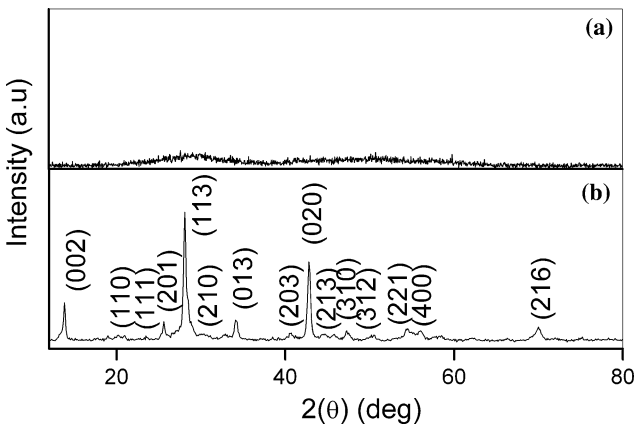

Fig. 1 XRD patterns for (a) the as-quenched glass plate; (b) the heat-treated (875 K/12 h > T_{cr} in DSC studies) CBBO glass plate

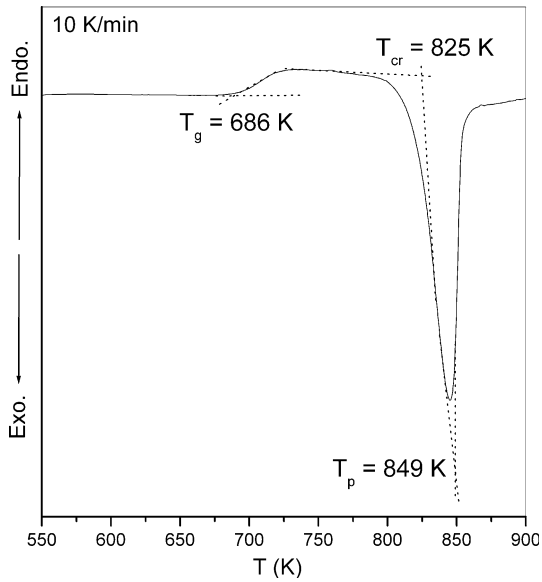

Fig. 2 DSC trace for the as-quenched $CaBi_2B_2O_7$ glass plate

Glass transition (T_g) analysis

The T_g dependence on the heating rate (α) has been analyzed using the following three different approaches. The empirical relation between the T_g and α according to Lasocka [15] is of the following form:

$$T_g = A_g + B_g \log \alpha \quad (1)$$

where A_g and B_g are the constants for a given glass composition at a particular temperature T. The constant B_g is related to the method of quenching the sample. Lower the cooling rate of the melt, lower the B_g value. It signifies the response of the configurational changes within the glass transition region to the heating rate. The plot of T_g and log α for the CBBO glass plate and a theoretical fit (solid line) are shown in Fig. 3. The inset in the figure shows clearly an upward shift in T_{gp} with increasing heating rate. The values that are obtained for A_g and B_g are 664 and 22 K, respectively, for CBBO glass. The above relation now can be written as

$$T_g = 664 + 22 \log \alpha \quad (2)$$

The second approach for rationalizing T_g or T_{gp} is based on the Kissinger's formula [13], in which the T_{gp} has a linear dependence on the heating rate, according to which

$$\ln\left(\frac{\alpha}{T_{gp}^2}\right) = \frac{-E_g}{RT_{gp}} + \text{const.} \quad (3)$$

where E_g is the activation energy associated with the glass transition and R is the universal gas constant. A plot of

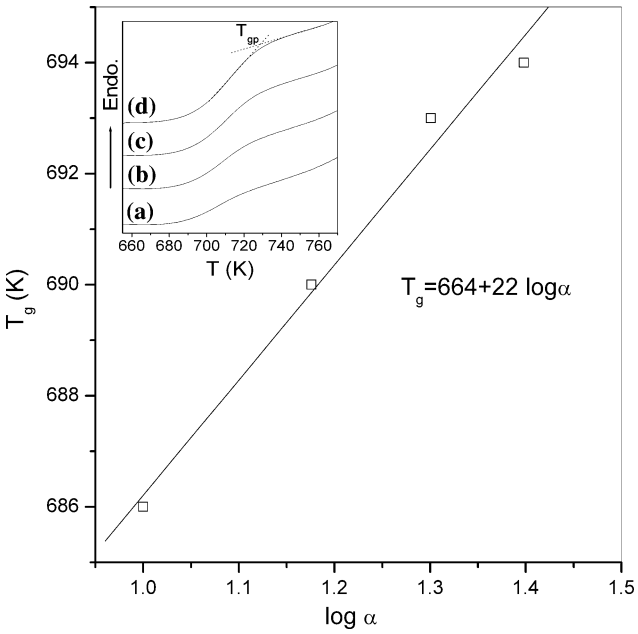

Fig. 3 T_g versus log α for the as-quenched CBBO glass plate and the inset depicts the glass transition peaks observed at heating rates of (a) 10 K/min, (b) 15 K/min, (c) 20 K/min, and (d) 25 K/min

$\ln(\alpha/T_{gp}^2)$ versus $(1000/T_{gp})$ gives a linear relation, which is depicted in Fig. 4. The experimental points of the present work along with a theoretical fit (solid line) to the above relation suggest its validity. From the slope of the straight line, the value for E_g is found to be 332 ± 5 kJ/mol.

The third approach, which is due to Moynihan et al. [14], is given by

$$\frac{\mathrm{d}\ln\alpha}{\mathrm{d}(1/T_{gp})} = -\frac{E_g}{R} \tag{4}$$

For Eq. 4, the necessary constraint is that prior to reheating, the glass must be cooled from above to well below the glass transition region at a rate which is either equal to or proportional to the reheating rate. In the present experiment, the sample is heated and cooled around the glass transition region in such a way that the cooling rate is equal to the reheating rate. A plot between ln α and $1000/T_{gp}$ is shown in Fig. 4. The value obtained for E_g from Fig. 4 is 327 ± 5 kJ/mol, which is in close agreement with that obtained by the Kissinger method.

Crystallization kinetics

Kinetic parameters (crystallization activation energy (E_{cr}) and Avrami exponent (n)) related to the glass crystallization process could be obtained from non-isothermal methods employing DSC experiments. Figure 5 shows the DSC traces (exothermic) obtained for the as-quenched CBBO glass plates at different heating rates (10, 15, 20, and 25 K/min). The systematic shift in the peak position with heating rate is tentatively attributed to thermal relaxation phenomena. The variation in peak temperature with heating rate is governed by the activation energy (E_{cr}) [13]. At higher heating rates, the activation energies involved would be higher as a result, the peak crystallization temperature shifts toward higher temperatures. Thus by monitoring the shift in the position of the exotherm as a function of the heating rate, one could obtain the kinetic parameters.

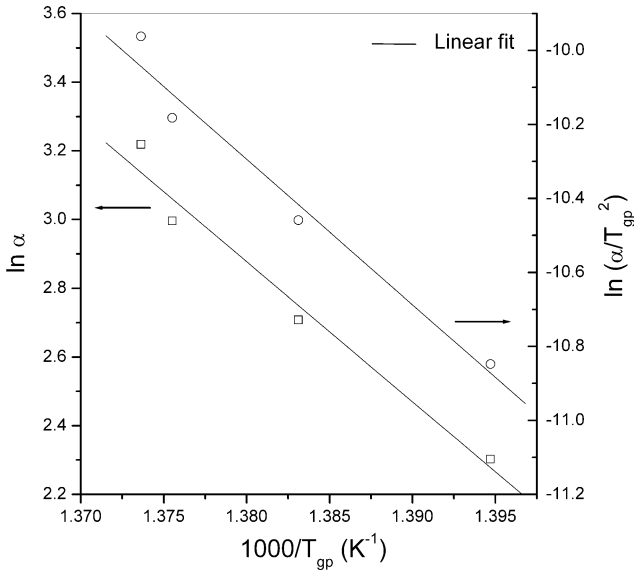

Fig. 4 ln(α) and $\ln(\alpha/T_{gp}^2)$ versus $1000/T_{gp}$ for the as-quenched CBBO glass plate

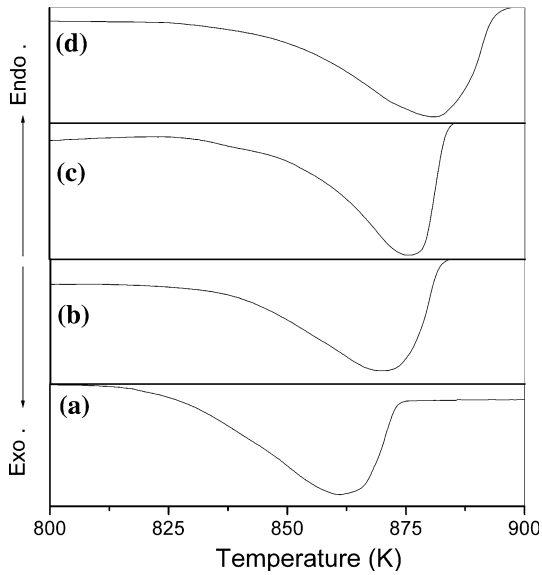

Fig. 5 DSC traces for CBBO glass plate at various heating rates: (a) 10 K/min, (b) 15 K/min, (c) 20 K/min, and (d) 25 K/min

For rationalizing heating rate dependent crystallization temperature, Lasocka [15] equation can be invoked, which is stated as

$$T_{cr} = A_{cr} + B_{cr} \log \alpha \quad (5)$$

where A_{cr} is the crystallization temperature for the heating rate of 10 K/min and B_{cr} is a constant. Figure 6 shows the plot between T_{cr} and log α (solid line is a linear fit) for the as-quenched CBBO glass plate. The above relation for CBBO glasses can be written as

$$T_{cr} = 746 + 79 \log \alpha \quad (6)$$

The above equation is the effective description of the dependence of T_{cr} on the heating rate for the as-quenched CBBO glasses.

The second approach that is adopted to analyze the T_{cr} is non-isothermal crystallization kinetics for the as-quenched CBBO glasses. Most of the techniques developed to study the crystallization kinetics based on the JMA equation [10–12] are essentially derived on the basis of experiments carried out under isothermal conditions.

To understand the nucleation and growth process under the non-isothermal crystallization kinetics, several theoretical methods [16] have been adopted based on the JMA equation. All the methods assume a constant heating rate, α, in the DTA or DSC experiments, in which

$$T = T_o + \alpha t \quad (7)$$

where T_o is the initial temperature (300 K), α is the heating rate, and T is the temperature after time t. The primary goal of these methods is to identify two parameters, the overall effective activation energy, E_{cr}, and the order of the reaction or Avrami exponent, n.

Determination of the crystallization activation energy

The crystallization activation energy could be extracted using the formula proposed by Augis and Bennet [17] as follows

$$\ln\left[\frac{\alpha}{T_p - T_o}\right] = \text{const.} - \frac{E_{cr}}{RT_p} \quad (8)$$

when $\ln[\alpha/(T_p - 300)]$ is plotted against $1/T_p$ (Fig. 7), a straight line is obtained with a slope $-E_{cr}/R$. The value of E_{cr} for the as-quenched CBBO glass by this method is 295 ± 5 kJ/mol.

Kissinger [13] formulated the method that is commonly used for analyzing crystallization data in DSC or DTA experiments, according to which,

$$\ln\left(\frac{\alpha}{T_p^2}\right) = \frac{-E_{cr}}{RT_p} + \text{const.} \quad (9)$$

Figure 8 shows the plot of $\ln(\alpha/T_p^2)$ versus $1000/T_p$. The value obtained for E_{cr} is 292 ± 5 kJ/mol, which is in close agreement with the value obtained by the Augis and Bennet method.

It is observed that the crystallization peaks are asymmetric in nature (Fig. 5) for the as-quenched CBBO glasses under study, implying that more than one process, i.e. both the surface and bulk crystallization process, may be active as the Avrami exponent 'n' varies between 1 and 4. It also could be due to a local phase separation because of the presence of Bi^{3+} and Ca^{2+} cations in the glass. Thus, to study the nature of the crystallization process, the fraction of crystallization (x) was determined. The fraction of crystallization (x) of the as-quenched glass during heating

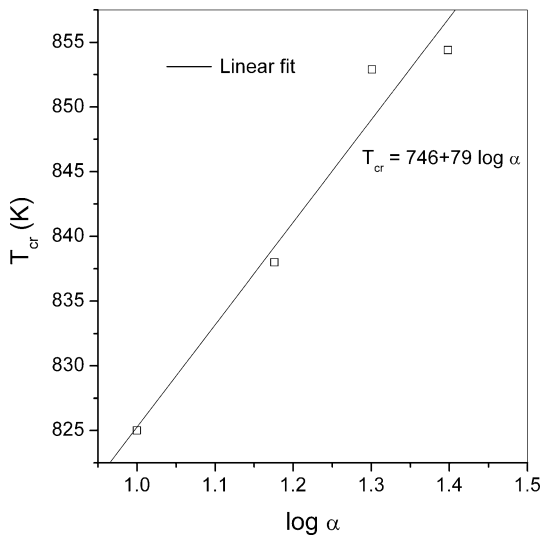

Fig. 6 T_{cr} versus log α plots for the as-quenched CBBO glass plate

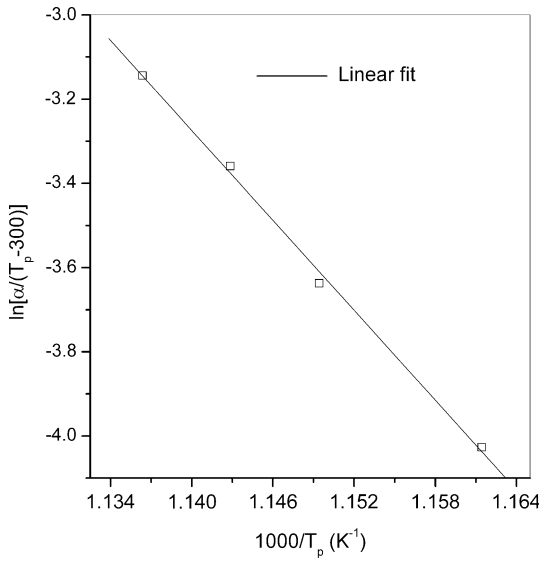

Fig. 7 $\ln[\alpha/(T_p - 300)]$ versus $1000/T_p$ for CBBO glass plate

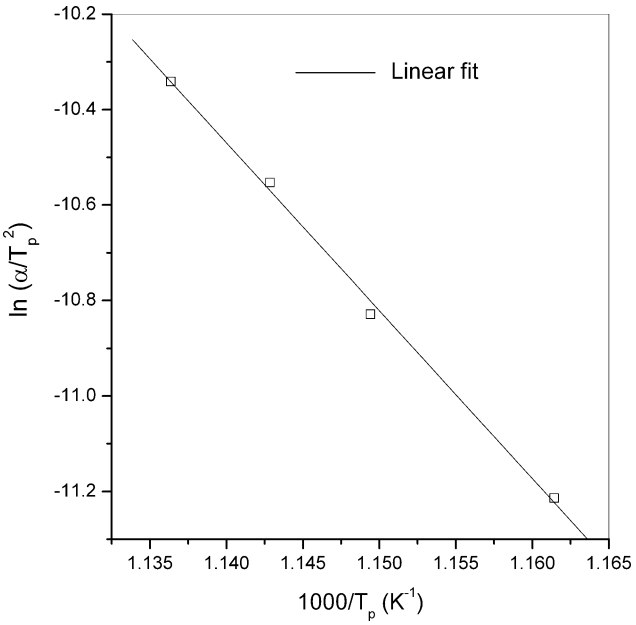

Fig. 8 $\ln(\alpha/T_p^2)$ versus $1000/T_p$ for the as-quenched CBBO glass plate

process could be obtained from the DSC data as a function of temperature (T) [18]. The fraction of crystallization (x) at any temperature T is given by $x = (A_x/A)$, where A is the total area under the exotherm between the temperature T_i, where the crystallization is just started and the temperature T_f, where the crystallization is completed, and A_x is the area between the initial temperature and a temperature, T, ranging from T_i to T_f.

Using the above technique, the fraction of crystallizations (x) was determined at different temperatures and heating rates for the as-quenched CBBO glasses. Figure 9 shows the typical sigmoidal curves for the fraction of crystallization (x) and temperatures (T) at various heating rates (10, 15, 20, and 25 K/min). To determine the value of Avrami exponent (n), $\ln[-\ln(1-x)]$ and $1000/T$ at different heating rates were plotted. Figure 10 shows the plots of $\ln[-\ln(1-x)]$ and $1000/T$ at different heating rates. It is noticed that in the entire range of temperatures, the plots are non-linear at all the heating rates under study. According to the modified Ozawa equation [19], the fraction of crystallization (x) and the temperature (T) for the as-quenched glasses could be related as

$$\ln[-\ln(1-x)] = -n\ln\alpha - 1.052(n-1)\frac{E_{cr}}{RT} + \text{const.} \quad (10)$$

where E_{cr} is the activation energy for the crystallization, n is the Avrami exponent, T is the temperature in absolute scale, and R is the universal gas constant. From the above equation, the plot of $\ln[-\ln(1-x)]$ and $1000/T$ should be straight line with the slope of $1.052(n-1)E_{cr}/R$, but under the present study these trends are found to be non-linear as

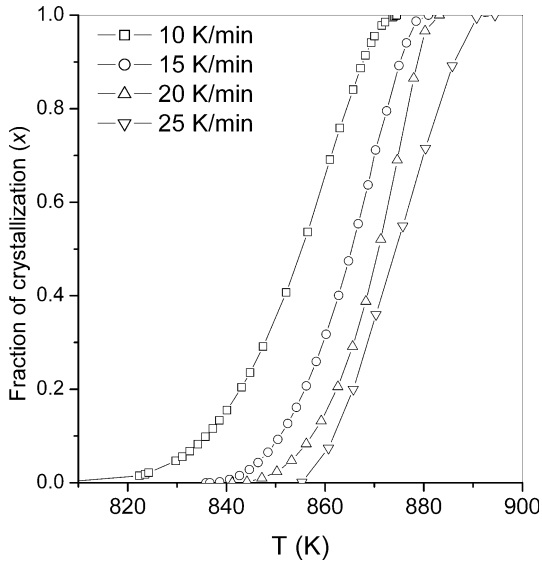

Fig. 9 Fraction of crystallization versus temperature curves at various heating rates for the as-quenched CBBO glass plate

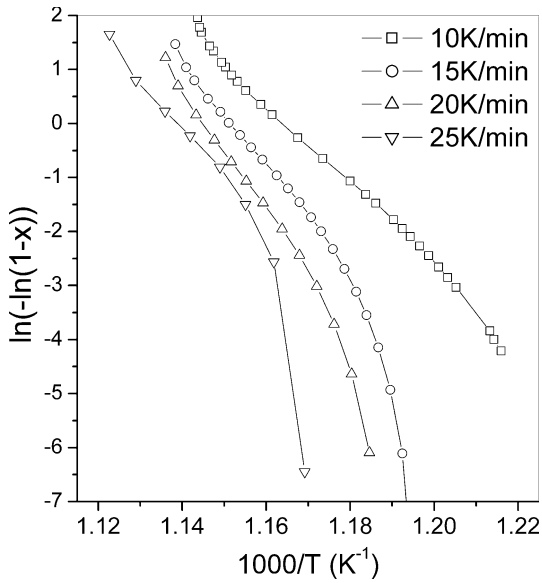

Fig. 10 Plot of $\ln[-\ln(1-x)]$ versus $1000/T$ for the as-quenched CBBO glass plate at various heating rate

shown in Fig. 10 at all the heating rates. It suggests that there is a variation in E_{cr} and n during crystallization process of CBBO glass plates. In the above context it is interesting to study the change in the activation energy and Avrami exponent during the crystallization of CBBO glasses.

Local activation energy

Generally, activation energy is defined as the threshold energy above which the fluctuation of energy in the

activation complex is sufficient for the elementary reaction to take place. The value of activation energy is constant and characteristic for each reaction. It is observed that in few glass systems, the activation energy is dependent on the fraction of crystallization [20–22]. So, a local activation energy $E_c(x)$, which represents the activation energy at a stage when the crystallized volume fraction is x, is applied to describe the variable activation energy which reflects the change of nucleation and growth behavior during crystallization process.

The calculation of the local activation energy $E_c(x)$ could be obtained using non-isothermal DSC experiments. The local activation energy ($E_c(x)$) for the crystallization of the as-quenched CBBO glass plates is determined using the method introduced by Ozawa [23], according to which

$$\left[\frac{\mathrm{d}\ln\alpha}{\mathrm{d}(1/T)}\right]_x = -\frac{E_{cr}(x)}{R} \tag{11}$$

where R is gas constant, T and α are the temperature and the heating rate corresponding to the value of x.

Using the experimental data that are depicted in Fig. 9, $\ln\alpha$ and $1/T$ is plotted at various values of x and the $E_{cr}(x)$ is obtained from the slope of the curve. Figure 11 shows the variation of the crystallized volume fraction and the local activation energy for the as-quenched CBBO glass plate. It is noticed that at the initial stages of crystallization process, the local activation energy of the crystallization of the as-quenched CBBO glass is 235 ± 5 kJ/mol ($x = 0.2$). When the crystallized volume fraction is in the range of 0.5–0.7, the local activation energy increases slowly and becomes almost constant (about 321 ± 5 kJ/mol). Beyond this point the local activation energy increases rapidly with the fraction of crystallization (x).

It is known that the local activation energy ($E_c(x)$) is composed of two parts: activation energy of nucleation (E_n) and the activation energy of growth (E_g) [24]. This could be expressed as:

$$E_c(x) = aE_n + bE_g \tag{12}$$

where a and b are two variables related to the Avrami parameter and $a + b = 1$. It is expected that at the beginning, the process of nucleation dominates ($b = 0$) and at the end of the crystallization, only the growth process ($a = 0$) is expected to dominate. As $x \to 0$, $E_c(x) \to E_n \approx 200 \pm 5$ kJ/mol and as $x \to 1$, $E_c(x) \to E_g \approx 375 \pm 5$ kJ/mol for the present glasses.

Avrami exponent

Lu et al. [21] introduced an equation in order to calculate Avrami exponent from the prior knowledge of local activation energy for non-isothermal crystallization process, which is expressed as

$$n(x) = \frac{-R\partial\ln[-\ln(1-x)]}{E_c(x)\partial\ln(1/T)} \tag{13}$$

Taking into account the local activation energy ($E_c(x)$), Avrami exponents ($n(x)$) at a heating rate of 10 K/min were calculated using the above equation (Eq. 13) for the as-quenched CBBO glasses. Figure 12 shows the variation of Avrami exponent with the fraction of crystallization (x) at a heating rate of 10 K/min. It is seen that the Avrami exponent decreases from 2.9 to 1.5 where the fraction of crystallization increases, indicating a change in the crystallization process from the two-dimensional bulk to surface crystallization [21].

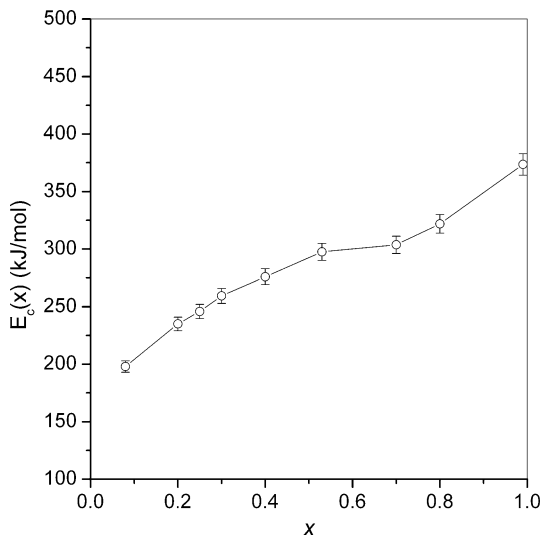

Fig. 11 $E_c(x)$ versus x for the as-quenched CBBO glass plate

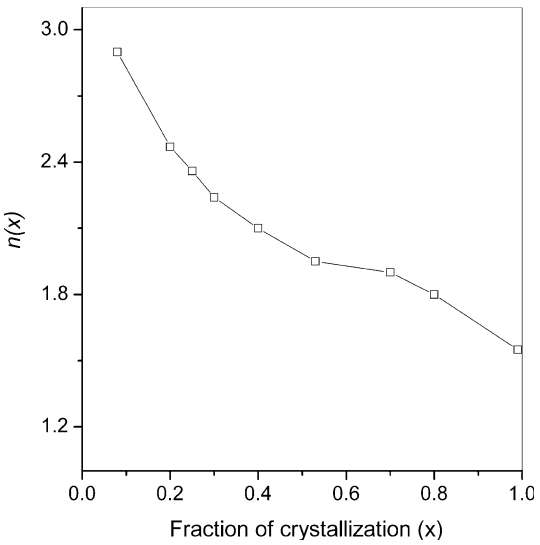

Fig. 12 The local Avrami exponent $n(x)$ as a function of crystallized fraction at a 10 K/min heating rate

Conclusions

The glass transition and crystallization behavior are rationalized in terms of Lasocka formulae. The crystallization parameters of CBBO glasses, which are scientifically important, have been evaluated using different methods derived from non-isothermal experiments. The average value of the crystallization activation energy is 295 ± 5 kJ/mol for CBBO glass plates. The local activation energy of the as-quenched CBBO glasses is determined and found to be varying with the fraction of crystallization (x). The activation energies for the nucleation and growth processes are calculated and found to be 200 ± 5 kJ/mol and 375 ± 5 kJ/mol, respectively. The crystallization process in CBBO glasses could be either bulk or surface, depending on the amount of fraction of crystallization.

References

1. Takahashi Y, Benino Y, Fujiwara T, Komatsu T (2001) J Appl Phys 89:5282
2. Murugan GS, Varma KBR, Takahashi Y, Komatsu T (2001) Appl Phys Lett 78:4019
3. Prasad NS, Varma KBR, Takahashi Y, Benino Y, Fujiwara T, Komatsu T (2003) J Solid State Chem 173:209
4. Barbier J, Cranswick LMD (2006) J Solid State Chem 179:3958
5. Ray CS, Zang T, Reis ST, Brow RK (2007) J Am Ceram Soc 90:769
6. Kissinger HE (1957) Anal Chem 29:1702
7. Ray CS, Fang X, Day DE (2000) J Am Ceram Soc 83:865
8. Ray CS, Yang Q, Huang W, Day DE (1996) J Am Ceram Soc 79:3155
9. Ray CS, Huang W, Day DE (1991) J Am Ceram Soc 74:60
10. Avrami M (1939) J Chem Phys 7:1103
11. Avrami M (1940) J Chem Phys 8:212
12. Avrami M (1941) J Chem Phys 9:177
13. Kissinger HE (1956) J Res Nat Bur Stand 57:217
14. Moynihan CT, Easteal AJ, Wilder J (1974) J Phys Chem 78:2673
15. Lasocka M (1976) Mater Sci Eng 23:173
16. Bansal NP, Doremus RH, Bruce AJ, Moynihan CT (1983) J Am Ceram Soc 66:233
17. Augis JA, Bennett JE (1978) J Therm Anal 13:283
18. Prasad NS, Varma KBR (2005) J Am Ceram Soc 88:357
19. Matusita K, Komatsu T, Yokota R (1984) J Mater Sci 19:291. doi:10.1007/BF02403137
20. Calka A, Radlinski AP (1988) Mater Sci Eng 97:241
21. Lu W, Yan B, Huang W (2005) J Non-Cryst Solids 351:3320
22. Lu K, Wang JT (1991) Mater Sci Eng A 133:500
23. Ozawa T (1986) J Therm Anal 31:547
24. Yinnon H, Uhlmann DR (1983) J Non-Cryst Solids 54:253